Coupled control of land use and topography on nitrate-nitrogen dynamics in three adjacent watersheds

Rui Jiang*[1, 2], Krishna P. Woli[2, a], Kanta Kuramochi[2], Atsushi Hayakawa[2, b], Mariko Shimizu[2], Ryusuke Hatano[2]

1. College of Resources and Environment, Northwest A&F University; Key Laboratory of Plant Nutrition and the Agri-environment in Northwest China, Ministry of Agriculture, Yangling 712100, China
2. Graduate School of Agriculture, Hokkaido University, Sapporo 060-8589, Japan

Abstract

To investigate the factors controlling nitrate-nitrogen (NO_3^--N) dynamics during snowmelt season and rainfall events, this study was conducted in three adjacent headwater stream watersheds with coupled land use and topography characteristics in eastern Hokkaido, Japan. The agriculture-dominated watershed (AW) had flat topography in agricultural area, the forest-dominated watershed (FW) was characterized by a steep slope in forest area, and the mixed agriculture-forested watershed (AFW) had flat topography in the agricultural area and steep topography in the forest area. Results showed that the timing of NO_3^--N export is different between the forested and steep watershed FW and the agricultural and flat watershed AW. The NO_3^--N export peaked before discharge peak with quick subsurface flow during snowmelt and

* Corresponding author. Phone: +86-29-87081581; Fax: +86-29-87080055; Email: jiangrui@nwsuaf.edu.cn ; Postal address: Room 218, College of Recources and Environment, Northwest A&F University, 3# Taicheng Road, Yangling, Shaanxi, 712100, China.

Present address: [a] Department of Natural Resources and Environmental Sciences, University of Illinois at Urbana-Champaign, Urbana, IL 61801, USA; and [b] Department of Biological Environment, Akita Prefectural University, Akita 010-0195, Japan

rainfall events in the AW, while after discharge peak with slow subsurface flow in the FW. The difference in the timing of NO_3^--N export is attributed to the subsurface flow which is regulated by the coupled characteristics of topography and land use. The fast release of NO_3^--N in the FW was attributed to the "flushing mechanism", which was driven by the rapid response of the subsurface flow due to the macropores in the forest soil and the steep slope. The AW showed a consistent "prolonged flush" of NO_3^--N, where NO_3^--N concentrations peaked after the peak of discharge, which might be attributed to the slow occurrence of subsurface flow because of the flat slope and the low hydraulic conductivity of the pasture. In the AFW, the NO_3^--N concentration peaked before the discharge peak during the snowmelt season but after the discharge peak during the rainfall events, indicating other factor such as the macropores related to the freeze/thaw cycles replaced of the coupled characteristics of topography and land use controlling the timing of NO_3^--N export in the mixed watershed.

Key Words

Nitrate-N export; rainfall events; snowmelt; subsurface flow

1. Introduction

Nitrogen (N) export from watersheds at different spatial and temporal scales, especially the estimation of hydrologically induced mobilization of nitrate-nitrogen (NO_3^--N) from forested watersheds, has received considerable attention in recent hydrological and biogeochemical studies (Rusjan et al., 2008; Christopher et al., 2008a; 2008b; Piatek et al., 2009; McNamara et al., 2008). During the rainfall events and snowmelt season, many studies have reported a significant increase in NO_3^--N, and they have attributed this increase to NO_3^--N flushing. Hydrological flushing of

NO_3^--N has been explained by the following: 1) a flushing mechanism, in which the flush of stream NO_3^--N, originates from a near-surface soil layer when the water table rises to the upper soil profile during hydrological events (Burns, 2005; Creed and Band, 1998; Jiang et al., 2010); 2) a draining mechanism, where recharge of groundwater due to snowmelt and precipitation translocates N from the upper layer of the soil profile into the deeper hydrological flow pathways that are released slowly over the year, either via displacement by infiltrating precipitation during the hydrological events or via groundwater discharge to the stream during baseflow (Creed and Band, 1996; McHale et al., 2002; Inamdar et al., 2004; Christopher et al., 2008a); and 3) a prolonged flushing mechanism, where flushing occurs throughout a storm, and the peak NO_3^--N concentration is reached with a time delay after the peak of the hydrograph graph (Rusjan et al., 2008).

However, hydrological controls on NO_3^--N flushing at the watershed scale are still poorly understood. Hydrological NO_3^--N flushing has shown variability in the timing of NO_3^--N export. For instance, Creed and Band (1998) and Zhang et al. (2007) observed a clockwise pattern between discharge and NO_3^--N concentrations, which means NO_3^--N peaked before the discharge peak. However, Rusjan et al. (2008) and Jiang et al. (2010) illustrated a counter-clockwise pattern of discharge and NO_3^--N concentrations, with higher NO_3^--N concentrations during the receding limb of discharge. The differences in the timing of the delivery of NO_3^--N to streams, depending on the location, seasons, and the antecedent moisture condition, have been related to the differences in the mechanisms that control the export of NO_3^--N (Wagner et al., 2008). Many studies have demonstrated that hydrological N export is complicated by a variety of factors, such as land use (Kaushal et al., 2008; Poor and McDonnell, 2007; Wagner et al., 2008; Vidon et al.,

66 2009), topography (Buttle et al., 2001; Creed and Band 1998; Creed and Beall, 2009; Inamdar and
67 Mitchell, 2006; Ogawa et al., 2006; Welsch et al., 2001; Bayabil et al., 2010; Chen et al., 2010),
68 hydrological characteristics (i.e., antecedent moisture condition, rainfall amount, and rainfall
69 intensity) (Zhang et al., 2007; Christopher et al., 2008a; Busjan et al., 2008), soil types
70 (McNamara et al., 2008), vegetation types (Christopher et al., 2006, 2008b; McNamara et al.,
71 2008), N source (Christopher et al., 2008a; Park et al., 2003), and climatic variables (Kaushal et al.,
72 2008; Mitchell et al., 1996; Park et al., 2003), all of which contribute to the heterogeneous spatial
73 and temporal patterns of NO_3^--N export.

74 For example, land use has been found to have a large effect on the quantity of N exported to
75 the stream. There is a significant correlation between N export and the percentage of agricultural
76 area in the watershed (Hayakawa et al., 2006; Woli et al., 2004). Land use can significantly affect
77 the watershed hydrological and N export responses to storm events, with higher NO_3^--N
78 concentrations in agriculture watersheds and lower in mixed agriculture/urban watershed (Vidon
79 et al, 2009). Poor and McDonnell (2007) examined the seasonality of the NO_3^--N dynamics in
80 three catchments with different land use patterns to explore how human activities altered the
81 export of NO_3^--N. Across a variety of land uses, Wagner et al. (2008) reported a variation in the
82 timing of NO_3^--N delivery to streams that was associated with the differences in the mechanisms
83 controlling the delivery of NO_3^--N to streams.

84 Topography may regulate the hydrologic flushing of NO_3^--N through its effects on the sources
85 of flushable NO_3^--N or the rate of expansion versus contraction of the variable source area (Creed
86 and Band, 1998). Catchments with larger, hydrologically organized variable source areas or a
87 greater potential for the lateral expansion of the source areas will have longer flushing times and

higher rates of N export. Topographic depressions and/or flatness, where NO_3^--N is transformed either into gaseous forms of N or into dissolved organic forms of N, can act as sinks for NO_3^--N (Creed and Beall, 2009). Topography may also affect the N export associated with soil moisture. Welsch et al. (2001) showed that the wetter areas of a catchment with a higher topography index value had higher NO_3^--N values than in drier locations. Although several studies have clearly documented the relationships between topography and watershed NO_3^--N concentrations/loadings, little is known about the effect of the topography on the timing of NO_3^--N export. Because the topography plays an important role in the generation of subsurface flow and determines when the subsurface flow occurs quickly enough to contribute to the peak stream discharge (Chen et al., 2010), the steep topography may result in a more rapid response of NO_3^--N flushing due to the quicker subsurface flow.

Moreover, these studies have shown that NO_3^--N export is not only one factor-controlling process, but it is also a function of the complex factors affecting the sources, transport, and transformations of N in a watershed, including the microbial transformation of N, plant uptake, N transport, hydrologic processes, climate, and landscape (topography, geology, soil depth, and land cover). Therefore, to improve upon the limited understanding of the factors controlling N export and their integrated effects, analysis of the temporal and spatial variables and the characterization of such heterogeneous landscapes are required.

In the Shibetsu watershed, located in eastern Hokkaido, Japan, N export was reported to have a significant relationship with land use (Hayakawa et al., 2006; Woli et al., 2004) and hydrological events (Jiang et al., 2010). The NO_3^--N export mechanism was described as flushing mechanism, which was closely related to subsurface flow (Jiang et al., 2010). However, the Shibetsu watershed

has coupled land use and topography characteristics. The upstream area is characterized by steep topography and is covered by forest, whereas the downstream area possesses gently sloping areas currently being used for agriculture. As mentioned above, land use may affect the N export mechanism, while topography may regulate the occurrence of subsurface flow. Hence, the flow system and N export mechanism may be different at spatial scale in Shibetsu area. How the land use/topography, especially the coupled characteristics effect on the subsurface flow and N export in Shibetsu area is not clear. To examine whether coupled topography and land use affect N export and to investigate the variation in those effects, we chose three adjacent watersheds with different land use types and topographies to examine the hydrological responses of NO_3^--N export, in particularly, the timing of NO_3^--N export associated with subsurface flow

2. Materials and Methods

2.1 Watershed description

Three headwater stream watersheds adjacent to each other (agriculture-dominated, AW; forest-dominated, FW; and mixed agriculture-forested, AFW), located in the Shibetsu watershed (43.634′N, 145.085′E) in eastern Hokkaido, Japan (Fig. 1), were selected for the study. In the Shibetsu area, the mean annual temperature is 5°C, and the average annual precipitation is 1,147 mm. The snowpack persists from early December to late April, with the annual maximum snowpack depth of 73 cm and annual snowfall of 480 cm. The soil freezing depths range from 35 to 50 cm. Stream discharge varies with seasons at the outlets of headwater streams and the Shibetsu watershed. Peak stream discharge occurs during the snowmelt season and again in August to November during rainfall events (1978-2002, Japan Meteorological Agency 2007,

http://www.jma.go.jp/jma/indexe.html).

The AW covers 14.3 km^2 and is located in the middle of the Shibetsu watershed (Fig. 1). The main land use is agriculture, accounting for 73.5% of the area (Table 1), and the other land uses are forest (23.5%), water (2.6%) and urban (0.4%). The soils are sandy loam Andosols with high sand (50%~77%) and low clay (<7%) contents. The AFW covers an area of 36.6 km^2 and consists of 58.9% of agriculture, 37.1% of forest, 2.6% of urban and 1.4% of water (Table 1). The soils are mainly loam, sandy loam, and loamy sand Regosolic and Cumulic Andosols (sand: 48-85%, silt: 10-42%, and clay: <10%). The FW has the largest area, 70.0 km^2, and is dominated by forest (84.4%, Table 1), with some agriculture (14.5%) and water (1.1%). It has Brown Forest soils with 55~58% of sand, 16~18% of silt, 18~21% of clay, and 5~7% of rock (soil data in AW, AFW and FW were from: http://www.agri.hro.or.jp/chuo/kankyou/soilmap/html/map_index.htm, government report data). The topographic characteristics were analyzed using GIS based on a 50 m digital elevation model (DEM). The overall relief of the AW is 132 m, ranging from 46 m to 241 m above sea level. The relief ratio (the difference between maximum and minimum elevation of a watershed divided by its maximum length of the river or stream) is 0.0146. The flat terrain (less than 5% of slope) accounts for 86.0% of the area, and it is connected to slight steeper near-stream zones (Fig. 1, Table 1). The relief of the AFW varies from 69 m to 575 m above sea level, with a mean value of 193 m and a relief ratio value of 0.0362. The flat topography (less than 5% of slope) dominates 60.2% of this watershed. The FW is located in a mountainous area with the highest relief of 977 m above sea level and a relief value of 0.0553, where 62.8% of the area is steep (larger than 10% of slope) and only 17.0% is less than 5% of slope. As illustrated in Fig. 1, land use and topography are coupled characteristics in the three headwater stream watersheds,

where forest covers the steep area and agriculture dominates the flat area. Grassland and pasture occupy 90% of the agricultural land. The major vegetation types are *Phleum pretense* in agriculture land and Japanese larch (*Larix kaempferi*) in the forest. The underlying rocks are mainly volcanic ash and Pumice (younger volcanic ash bed) for the three watersheds (http://iggis1.muse.aist.go.jp/en/top.htm). For river areas, there are sand and gravel (alluvial deposits or Nita sand bed or Chashikotsu formation) in the three watersheds as well as green tuff, propylite and pumiceous tuff in FW and quartz bearing hypersthene andesite in AW. In FW, the bedrocks in mountainous areas are covered by sand, gravel and liparite, and the near river areas are hypersthene dacite.

2.2 Watershed monitoring, sampling, and analysis

Water samples were collected by an automated water sampler (ISCO 6712, Isco, Lincoln, NE, USA), which was installed at the outlet of each stream during hydrological events. The auto-sampler was triggered when rainfall was >4 mm 30 min^{-1}, with sampling intervals of 15 min to 1 h for the rising stage of discharge and 2 to 6 h for the receding stage. Twenty rainfall events were sampled for the three watersheds during 2003 to 2005. Water samples were collected during the snowmelt season in 2004 and 2005, and the sampler was triggered manually, with a sampling interval of 12 h. The water samples were transported to the laboratory immediately after collection and then stored at 4˚C until analysis. Rainfall was measured by a tipping-bucket rain gauge (0.2 mm) placed in an open area near the automated sampler. Stream discharge rates at baseflow were measured using a flow velocity meter (TK-105; Toho Dentan, Tokyo) at the outlets of the watersheds. The discharge rates were calculated by multiplying the sectional area of the stream by the flow velocity along a transect across the stream. The daily stream water level was determined

from water level data recorded every 15 min by water sensors equipped with data loggers (MC-1100W, STS, Sirnach, Switzerland). Daily discharge was calculated from daily stream water level using calibrated H-Q equations (quadratic curve) modeling the relationships between discharge (Q) and water level (H) (Tachibana and Nasu, 2003). Meteorological data were obtained from the Japan Meteorological Agency (http://www.jma.go.jp/ima/indexe.html). Groundwater wells in near-stream zones located in the FW (in forest area) and AW (in agricultural area) were constructed of 5 cm (ID) PVC pipes and groundwater levels were recorded using pressure transducer and capacitance water level probes at 1 hour intervals from March of 2003 to November of 2004. The shallow groundwater wells in the FW and AW were cored to the depth of 1.52 and 2.94 m, respectively, under the ground surface where a coarse sandy sediment layer (confined layer) was intersected. The deep groundwater wells in the FW and AW with a depth of 9.73 m and 12.52 m drilled through the confined layer and were cored to the aquifer of Mashu pumice layer (impermeable layer). Since the deep groundwater wells were located near the recharge area of confined groundwater, so the deep groundwater table (pressure) could be measured. However, the water level probes in deep groundwater wells didn't work well, so the data collection from two deep groundwater wells was actually from March to June 2004.

After filtering through 0.2 μm membrane filters, water samples were analyzed for NO_3^--N and Si. Nitrate-N concentrations were determined using ion chromatography (QIC Analyzer; Dionex, Sunnyvale, CA, USA); Si concentrations were determined colorimetrically using the molybdenum blue method.

2.3 Data analyses

Antecedent precipitation index

To estimate the pre-event soil moisture of the watershed, previous reports (Christopher et al., 2008a; Jiang et al., 2010; Rusjan et al., 2008) have used the antecedent precipitation index (API) as its indicator. The API for x preceding days is defined as follows:

$$API_x = \sum_{i=1}^{x} \frac{p_i}{i},$$

where x = 7 or 21 days before a rainfall event and P_i (mm) is the total precipitation on the i^{th} day before the event. We used API_7 to calculate the surface soil moisture and API_{21} for the shallow groundwater condition because the surface volcanogenous soil usually has high infiltration rates and water can move quickly into the shallow groundwater aquifer. However, the shallow groundwater needs long time to seep into the deep aquifer.

Runoff coefficient

The runoff coefficient (RC) is another indicator of wetness in a watershed and is defined as the total volume of discharge divided by the total volume of precipitation. The RCs for observed rainfall events were computed to estimate the differences in the runoff generation process influenced by the interactions of hydrological, biogeochemical, and transpiration processes in a watershed.

The timing of NO_3^--N export

Several studies have used clockwise or counter-clockwise patterns between discharge and NO_3^--N concentrations to show the timing of NO_3^--N export during hydrological events (Rusjan et al., 2008; Jiang et al., 2010; Creed and Band, 1998; Zhang et al., 2007). In this study, we used the clockwise or counter-clockwise patterns to examine the NO_3^--N flushing before or after the discharge peak during the snowmelt season. To find the variations in NO_3^--N concentrations in discharge during rainfall events, the NO_3^--N concentrations were plotted against time. The time

scale was first expressed as the time since the beginning of rainfall and then calculated as a multiple of the time to peak discharge rate (*Tp*). For example, the time since the beginning of rainfall at peak discharge is 3 h, and the duration at NO_3^--N peak is 6 h; thus, the time in multiples of *Tp* at the NO_3^--N peak is 2T*p*, and 1*Tp* is the time at peak discharge. This allowed the comparison of the variations in the NO_3^--N concentrations between the rainfall events in relationship to their *Tp*, and it provided a more uniform scale for comparing different rainfall events with extreme variations in discharge (Pathak et al., 2004; Han et al., 2010). In our study, we used the time in multiples of *Tp* to investigate the timing of NO_3^--N export associated with discharge. If there were several peaks in NO_3^--N concentration during a rainfall event, we defined the peak concentration of NO_3^--N as the largest one.

3. Results

3.1 Climatic characteristics

Table 2 shows that the rainfall in 2003 was larger than in normal years (30-yr average). During the study period, the lowest annual snowfall was in 2005, whereas the largest snowpack depth was in 2004.

3.2 Concentration-time relationships of NO_3^--N during hydrological events

Snowmelt season

Figure 2 shows that the peak discharge in 2004 was larger than that in 2005 for all three headwater stream watersheds because the snowpack depth was larger in 2004 than in 2005. Similarly, the peaks in NO_3^--N concentrations were much higher in 2004. The discharge peaks were observed earlier and were much lower in the AW than that in the AFW and FW, possibly because of the

242 watershed size. However, the NO_3^--N concentrations followed the opposite pattern and were
243 higher in the AW than that in the AFW. Although we only had the data for the groundwater tables
244 in AW and FW in 2004, the results showed that the NO_3^--N concentrations increased with the
245 increase of shallow groundwater table in AW and FW; the Si concentrations peaked with the peak
246 of deep groundwater table. The deep groundwater table increased after the shallow groundwater
247 table and then decreased slowly. The increased shallow and deep groundwater tables indicated that
248 the lateral and vertical movements of snowmelt water occurred synchronously, but the percolation
249 process needed a certain time. The concentrations of NO_3^--N and Si and groundwater tables all
250 peaked before the discharge peaked in the FW while after discharge peaked in the AW. The trends
251 of groundwater tables and Si concentrations suggested both shallow and deep groundwater might
252 contribute to NO_3^--N export during snowmelt season. Shallow groundwater table peaked before
253 discharge peak in the FW but after discharge peak in the AW, indicating subsurface runoff
254 occurred earlier in the AW than that in the FW, which may be attributed to the soil characteristics
255 such as the water conductivity or the macroporosity.

256 *Rainfall events*

257 Table 3 shows that the hydrological characteristics of the selected rainfall events varied
258 considerably. The total amount of rainfall ranged from 10 to 91 mm. Each watershed had rainfall
259 events from large (≥ 50 mm), moderate (20 mm < total rainfall < 50 mm) and small quantities of
260 rainfall (≤ 20 mm) and at both the dry and wet antecedent soil moisture conditions (API_7 ranged
261 from 0 to 24.18, and API_{21} was from 2.42 to 28.81). Regardless of the difference in the
262 characteristics of rainfall events, the runoff coefficient showed smaller values in the AW and larger
263 values in the FW, suggesting that the generation of runoff may be controlled not only by

hydrological characteristics, but also by watershed characteristics such as the land cover, slope, watershed size, or soil type.

Figure 3 shows the different patterns of the NO_3^--N concentrations during rainfall events in the three watersheds. In the FW, the NO_3^--N concentrations had similar trends with shallow groundwater table, both of which increased with the rising limb of discharge and peaked before the discharge peak (Fig. 3a). However, the shallow groundwater increased slowly after discharge peak in the AW (Fig. 3c); the NO_3^--N concentrations first decreased with the discharge peak and then increased with the increase of shallow groundwater table after discharge peak. In the AFW and AW, the NO_3^--N concentrations showed several peaks, with the largest one occurring after the discharge peak (Fig. 3b, c). The peak concentrations of NO_3^--N ranged from 0.31 to 0.80, 1.07 to 1.76, and 1.62 to 1.98 mg L^{-1} in the FW, AFW, and AW, respectively (Table 4). The Si concentrations decreased when the discharge peaked, and opposite trajectories were found for NO_3^--N and Si concentrations for all three watersheds (Fig. 3).

3.3 Nitrate-N export patterns during hydrological events

Snowmelt season

The relationships between discharge and NO_3^--N concentrations during the snowmelt season are given in Fig. 4. The direction of all relationships in the FW and AFW was clockwise patterns, indicating that higher NO_3^--N concentrations were observed during the rising limb of discharge, whereas in AW, NO_3^--N consistently displayed a counter-clockwise hysteresis, with higher concentrations during the receding limb of discharge.

Rainfall events

Figure 5 shows the NO_3^--N concentration dynamics versus time in multiples of *Tp*. During all

rainfall events in the FW, the NO_3^--N concentrations increased sharply during the rising limb of discharge (peaked before 1 *Tp*). Table 4 shows that higher peaks in NO_3^--N concentrations were observed during the rainfall event on 26 July 2005, which had a high quantity of rainfall, and that lower peaks were during the smaller rainfall events on 8 and 25 August 2003. However, the small rainfall events with a high antecedent soil moisture condition showed a considerably higher peak in NO_3^--N concentration, as in the rainfall event on 15 November 2004. The AFW showed several peaks before or after 1 *Tp* for NO_3^--N concentrations during each rainfall event; however, the largest peak was observed at or after 1 *Tp* (the values of the time in multiple of T*p* were equal to or larger than 1, Table 4). The higher NO_3^--N concentrations were observed in large rainfall events (20 June 2003) or rainfall events with a high value of API_x (26 September 2003). In the AW, the NO_3^--N concentrations often decreased during the rising limb of discharge (before 1 *Tp*) and peaked after 1 *Tp*.

We analyzed the relationships between the time in multiples of *Tp* when NO_3^--N peaked or the peak NO_3^--N concentrations (in Table 4) and the rainfall amount, API_X, and RC (in Table 3). Significant correlations were found between API_X and the peak NO_3^--N concentrations (API_7: 0.85, $P<0.05$; API_{21}: 0.81, $P<0.05$) or the time in multiples of *Tp* when NO_3^--N peaked (API_7: 0.85, $P< 0.05$) in the AFW. The RC showed a significant negative correlation with the peak NO_3^--N concentrations (-0.80, $P< 0.05$) in the FW, suggesting the impact of streamflow dilution. There is no correlation in the AW. These results indicated that factors other than antecedent soil moisture condition control on NO_3^--N export in the AW and FW. An exponential relationship was found between the time in multiples of *Tp* when NO_3^--N peaked and the relief ratio for all three watersheds (Fig. 6). For the peak concentrations of NO_3^--N, there was a significant correlation

with the percentage of agricultural area in the watershed (Fig. 7). These results indicated that the NO_3^--N export among the three watersheds was different in both the export patterns (the timing of peak) and the peak concentrations. These differences in the timing of the NO_3^--N export and concentrations might be controlled by different watershed factors, such as topography and land use.

4. Discussion

The differences of NO_3^--N concentrations during snowmelt and rainfall events were significant among three watersheds ($P<0.01$). The NO_3^--N concentrations were much higher in the AW than that in the FW (Fig. 2, 3, Table 4), and there was a significant positive correlation between agricultural area and the peak NO_3^--N concentrations during the rainfall events (Fig. 7). These results are consistent with the previous findings that the N exports at the watershed scale increased with the percentage of agricultural area in a watershed used (Hayakawa et al., 2006; Kaushal et al., 2008; Woli et al., 2002; 2004). Land use affects the magnitude of N exported from the watershed that is associated with different N sources. Atmospheric N has been considered to be a major source of stream NO_3^--N in forested watersheds (Driscoll et al., 2003; Galloway et al., 2003; Park et al., 2003). Shibata et al. (2001) found that the NO_3^--N export in forest streams was as low as 0.5 mg L^{-1} in the eastern part of Hokkaido, which was consistent with the low N deposition in this area. Therefore, the low NO_3^--N concentration in the FW might be because of the low atmospheric N inputs. Hokkaido is the primary dairy farming area in Japan, and approximately 93% of livestock waste is used as organic fertilizer for grassland/pasture (Hokkaido Government, 1996). Higher N application rates in the form of chemical fertilizer and manure in agricultural areas have

330 resulted in surplus N as high as 49 kg N ha^{-1} yr^{-1} in the uplands of the Shibetsu watershed and the
331 NO_3^--N export in stream accounted for 14% of net N input (Hayakawa et al., 2009). Thus, the
332 large inputs of N to the agricultural land would lead to high NO_3^--N export in the AFW and AW.
333 Previous studies reported a significant correlation between N concentrations and discharge, but
334 the relationship varied widely depending on the study sites and the properties of the rainfall events
335 (i.e., Ahearn et al. 2004; McNamara et al. 2008; Christopher et al., 2008a; Zhang et al., 2007). For
336 a given watershed, hysteresis patterns are associated with the antecedent moisture condition of the
337 watershed. The antecedent wet condition was reported to result in the peak in NO_3^--N
338 concentration occurring before the discharge peak, whereas dry antecedent soil moisture was
339 related to the NO_3^--N flush occurring after the discharge peak (Christopher et al., 2008a; Jiang et
340 al., 2010; McNamara et al., 2008). In our study, the NO_3^--N concentration peak time only had
341 some relationship with API_X in the AFW, while consistent patterns of NO_3^--N export with
342 discharge were found within each watershed during the rainfall events (Fig. 5). This result
343 suggested that factors other than antecedent soil moisture condition were more important in
344 controlling the timing of NO_3^--N export among the watersheds. The topography was likely to
345 regulate the NO_3^--N concentration peak time, as the relief ratio was found to have an exponential
346 relationship with the NO_3^--N peak time (as a function of the peak discharge rate, Fig. 6). The steep,
347 forested watershed may cause the NO_3^--N to flush quickly and peak before 1 *Tp* during the rainfall
348 events or to have a clockwise pattern for the relationship between NO_3^--N concentration and
349 discharge during the snowmelt season. In contrast, the agricultural or flat watersheds may export
350 NO_3^--N more slowly and peak after 1 *Tp* or exhibit the counter-clockwise patterns. The
351 topography is thought to determine whether subsurface flow occurs quickly enough to contribute

352 to the peak stream discharge (Beven and Kirkby, 1979). Chen et al. (2010) also observed that
353 topography played a dominant role in the formation of the runoff components. When the
354 catchment mean slope increased by 87% (reduce the basin average topographic index from 14.14
355 to 13.43), the subsurface storm flow could increase by 50%, whereas overland flow decreased by
356 7.5% and baseflow by 6.7% (Chen et al., 2010). In Shibetsu watershed, the NO_3^--N export is
357 described as a flushing mechanism during storms, which the NO_3^--N flushed by subsurface runoff
358 with the rising shallow groundwater table (Jiang et al., 2010). We found the NO_3^--N concentration
359 always increased with the increase of shallow groundwater table (Fig. 3). Thus the topography is
360 likely to regulate not only the occurrence of subsurface flow but also the timing of NO_3^--N export.
361 However, the topography (relief ratio) could only explain 39% of the variation in the NO_3^--N peak
362 time (Fig. 6) for our watersheds. Thus, topography together with other factors should be taken into
363 account for clarifying the relationships between the stream discharge and the NO_3^--N
364 concentrations, such as the N sources, runoff, flow path, geology, soil, or land use (Chen et al.,
365 2010; Bayabil et al., 2010).

366 Some studies have found significant influence of land use on near surface hydrological
367 processes, especially when comparing forest and pasture (Germer et al., 2010; McDowell et al.,
368 2003; Alegre and Cassel, 1996), which may also explain the variability in the difference in the
369 timing of the NO_3^--N export between the AW and AFW (dominated by pasture/grassland) and the
370 FW (dominated by forest). According to the soil attributes and the geology of Shibetsu watershed,
371 the occurrence of subsurface flow could more depend on the shallow groundwater table, because
372 the shallow groundwater table is always high during snowmelt season and summer rainy season.
373 When the shallow groundwater tables rise high enough to subsurface soil layer during

hydrological events (the shallow groundwater tables always raise to subsurface soil layer as shown in figure 2 and 3a,3c), the subsurface flow could enhance. Therefore, the infiltration rate of water from soil to shallow aquifer could affect on the timing of subsurface flow occurrence (quick or slow). The underlying of the three watersheds is mainly volcanic ash with the same infiltration rate, so the water infiltration rate in soil may be different between forested and agricultural land use. For example, installation of pasture and cattle trampling increase bulk density and penetration resistance and reduce macroporosity, infiltration rates and hydraulic conductivity, which may result in slow subsurface flow/return flow in the pasture (Germer et al., 2010). In forested catchments of temperate regions, substantial subsurface flow can be generated because of the high infiltration capacities of the forest surface soils perched above less permeable soil layers or a slowly moving wetting front (Hammermeister et al., 1982). Moreover, live or decayed plant roots may form macropores easily in forest soil (Beven and Germann, 1982). Mosley (1982) showed under experimental conditions using forest soil, under both saturated and unsaturated conditions, that water could move downslope through macropores very rapidly. In the saturated zone, the fast response would depend on steep slopes and high hydraulic conductivity caused by macropores (Beven and Germann, 1982). Thus, the rapid subsurface flow/preferential flow/return flows from the macropores were common in the forest (Germer et al., 2010). In our study, the macropores would also cause high infiltration rate and so that the shallow groundwater table might rise quickly and then lead to fast subsurface flow. The response of the subsurface flow may be more significant because of the steep slope. In addition, the soil depth was thicker in the flat pasture/grassland than that in the steep forest in our study, which was similar to the study conducted in South China (Chen et al., 2010). Chen et al. (2010) reported that the watershed with a steeper slope and thin

soil deposits generated more subsurface flow and a larger proportion of quick flow than did the watershed with gentle slope and thick soil deposits. We observed the shallow groundwater table peaked before the discharge peak in the FW while after discharge peak in the AW (Fig. 3), which is a strong evidence to show the quicker subsurface flow in the forested steep watershed.

The timing of the NO_3^--N export for the snowmelt season in the AFW was different from that seen for the rainfall events. The NO_3^--N peaked before the discharge peak during the snowmelt season, but after the discharge peak during rainfall events. This may be because of an integrated effect of the mixed land use and mixed topography characteristics. However, the integrated effect was probably regulated by the macropores due to freeze/thaw cycles. Maximum soil freezing depths of 35-50 cm have been recorded in eastern Hokkaido, probably due to the lack of snow cover (Takeuchi 1980; 1981). Ou et al. (1999) showed that freeze/thaw could cause macropores and preferential flow in the soil. Thus, the increased macropores during the snowmelt season might make the NO_3^--N release more quickly. The result suggested, when the topography and land use are no longer the main characteristics in the mixed watershed, other factors such as the hydrological process related to macropores or the antecedent soil moisture (i.e., the correlation between API_X and the timing of NO_3^--N peak in AFW) would take control on NO_3^--N export.

The relationship between discharge and NO_3^--N concentrations in the FW, in which the NO_3^--N concentration peaked before the discharge peak, during the snowmelt season (Fig. 4) and rainfall events (Fig. 5); the inverse patterns of NO_3^--N and Si concentrations (Fig. 2, 3); and the similar patterns of NO_3^--N concentrations and shallow groundwater table (Fig, 2, 3) indicated that the supply of NO_3^--N accumulated near or at the soil surface was quickly flushed in response to the discharge hydrograph. This characteristic behavior has been termed the “flushing effect” or

418 flushing mechanism. Creed and Band (1998) stated that the NO_3^--N leached from the near-surface
419 soil layers by the rising of the water table was followed by a quick lateral transport of the leached
420 NO_3^--N to the stream via subsurface flow from the nitrate source areas. This flushing depended on
421 the variable source area, ascribed to topography through its effects on the source of flushable
422 NO_3^--N, or on the rate of expansion versus contraction of the variable source area (Creed and
423 Band, 1998).

424 The delayed peak of NO_3^--N (after 1Tp) in AW during the hydrological events (Fig. 3, 5) could
425 suggest that intensive NO_3^--N flushing occurred during the recession limbs of the peak discharge
426 and that the rapid runoff component was not the prevailing contributor to NO_3^--N export (Butturini
427 et al., 2006). As discussed above, this delayed peak may be related to the slower subsurface
428 flow/return flow due to the interplay of the flat topography and agricultural land use. There is also
429 likely to be a mechanism that controls the temporal mobilization of NO_3^--N on a watershed level
430 beyond the interactive behavior of the hydrological and biogeochemical settings (Rusjan et al.,
431 2008). Rusjan et al. (2008) explained that more accumulated NO_3^--N becomes mobilized
432 throughout the process of the rising of the saturation zone toward the upper soil layers enriched by
433 an accumulated NO_3^--N pool. In the time of the maximum extension of the variable source areas,
434 which can be shown as the hydrograph peaks, the maximum concentrations of NO_3^--N were still
435 not reached. This could be the result of the NO_3^--N moving slower from the variable source areas
436 and the surrounding hillslopes; thus, the mechanism has been called “prolonged nitrate flushing”.
437 Rusjan et al. (2008) found that the low hydraulic conductivity of the clay and silt soils in a
438 forested watershed in the southwestern part of Slovenia was the cause of the prolonged lateral
439 extension that they observed. Jiang et al. (2010) also observed that NO_3^--N concentrations peaked

after the peak of discharge in the Shibetsu watershed in 2003, but they attributed this to the low rate of change in the variable source area because of the low antecedent shallow groundwater level. In this study, the change in the variable source area and the response of subsurface flow may both be regulated by the flat topography in the AW, where we observed the slowly increase of shallow groundwater table after discharge peak (Fig. 3c).

In addition, the high concentrations of NO_3^--N and the similar trends with Si concentrations and the deep groundwater table at the beginning of the snowmelt and rainfall events (Fig. 2, 3) suggested that the source of NO_3^--N was groundwater, because the concentrations of Si and NO_3^--N were both very low in the rainwater samples in our study. As Iqbal (2002) reported, the geology that is favorable for vertical recharge during snowmelt/rainfall events creates fluid pressure within the aquifer, forcing groundwater to discharge laterally into the stream. Shibetsu watershed is mainly covered by volcanic soil, which has high water conductivity and the snowmelt/rainfall water always percolate to deep groundwater. Thus the "displacement of groundwater" caused NO_3^--N flushing at the beginning of the rainfall and formed the first peak of NO_3^--N in our study.

5. Summary and Conclusion

In this study, we explored the factors controlling the export of stream NO_3^--N, in three headwater stream watersheds to explain the large variation in N concentrations and the timing of NO_3^--N export on different temporal and spatial scales. Our results showed that the integrated effects of land use and topography probably regulated the timing of the NO_3^--N export (i.e., whether NO_3^--N flushing occurred before or after the discharge peak). The NO_3^--N in the FW was

462 exported more quickly because the watershed had both forest and steep topography, which may
463 produce subsurface flow more quickly than the agricultural watershed with flat topography. The
464 export mechanism of NO_3^--N was similar to the "flushing mechanism" that was related to
465 subsurface flow (Creed and Band, 1998). However, the slow response of the subsurface flow in
466 the AW, due to the pasture/grassland land use and flat topography, was likely to cause a
467 "prolonged flushing mechanism" for NO_3^--N export, such that the peak NO_3^--N concentration is
468 reached with a time delay after the hydrograph peak (Rusjan et al., 2008). Meanwhile, we noticed
469 in the mixed agriculture-forested watershed, other factors such as the macropores due to
470 freeze/thaw cycles might change the patterns of NO_3^--N export.

471 Although our watersheds had the coupled characteristics of land use and topography that were
472 very difficult to separate, if we looked at the factors controlling stream N export, we found an
473 integrated impact of land use and topography on the timing of NO_3^--N export related to subsurface
474 flow. Although we investigated the shallow groundwater table during snowmelt and rainfall events,
475 further study should examine the flow paths with more details, especially the subsurface flow, and
476 how the subsurface flow responds to the hydrological events through the macropores.

477

478 **6. Acknowledgements**

479 We thank Dr. Toshiya Saigusa, Mr. Osamu Sakai, Mr. Hiroyuki Koda, and Mr. Toshinobu Koba,
480 Hokkaido Konsen Agricultural Experiment Station, for their help and suggestions on this study.
481 This study was partly supported by a Japanese Grant-in-Aid for Science Research from the
482 Ministry of Education, Culture, Sports, Science and Technology (No.14209002 and No.19201008)
483 and The Strategic International Cooperative Program "Comparative Study of Nitrogen Cycling

484 and Its Impact on Water Quality in Agricultural Watersheds in Japan and China" by the Japan
485 Science and Technology Agency. The research grant was provided by the "Hokkaido Regional
486 Development Bureau for the Restoration Project in the Shibetsu River".

487

488 **7. References**

489 Ahearn, D.S., Sheibley, R.W., Dahlgren, R.A., Keller, K.E., 2004. Temporal dynamics of stream
490 water chemistry in the last free-flowing river draining the western Sierra Nevada, California.
491 J. hydrol. 295, 47-63.

492 Alegre, J.C., Cassel, D.K., 1996. Dynamics of soil physical properties under alternative systems to
493 slash-and-burn. Agr. Ecosyst. Environ. 58, 39-48.

494 Bayabil, H.K., Tilahun, S.A., Collick, A.S., Yitaferu, B., Steenhuis T.S., 2010. Are runoff
495 processes ecologically or topographically driven in the (sub) humid Ethiopian highlands? The
496 case of the Maybar watershed. Ecohydrology 3, 457-466.

497 Beven, K., Germann, P., 1982. Macropores and water flow in soils. Water Resour. Res. 18 (5),
498 1311-1325.

499 Beven, K.J., Kirkby, M.J., 1979. A physically based, variable contributing area model of basin
500 hydrology. Hydrol. Sci. Bull. 24, 43-69.

501 Burns, D.A., 2005. What do hydrologists mean when they use the term flushing? Hydrol. Process.
502 19, 1325-1327.

503 Buttle, J.M., Lister, S.W., Hill, A.R., 2001. Controls on runoff components on a forested slope and
504 implications of N transport. Hydrol. Process. 15, 1065-1070.

505 Butturini, A., Gallart, F., Latron, J., Vazquez, E., Sabater, F., 2006. Cross-site comparison of

506 variability of DOC and nitrate c–q hysteresis during the autumn–winter period in three
507 Mediterranean headwater streams: a synthetic approach. Biogeochemistry 77, 327-349.
508 Chen, X., Cheng, Q., Chen, Y.D., Smettem, K., Xu, C., 2010. Simulating the integrated effects of
509 topography and soil properties on runoff generation in hilly forested catchements, South
510 China. Hydrol. Process. 24, 714-725.
511 Christopher, S.F., Mitchell, M.J., McHale, M.R., Boyer, E.W., Burns, D.A., Kendall, C., 2008a.
512 Factors controlling nitrogen release from two forested catchments with contrasting
513 hydrochemical responses. Hydrol. Process. 22, 46-62.
514 Christopher, S.F., Page, B.D., Campbell, J.L., 2006. Contrasting stream water NO_3^- and Ca^{2+} in
515 two nearly adjacent catchments: the role of soil Ca and forest vegetation. Global Chang.
516 Biol. 12, 364-381.
517 Christopher, S.F., Shibata, H., Ozawa, M., Nakagawa, Y., Mitchell, M.J., 2008b. The effect of soil
518 freezing on N cycling: Comparison of two headwater subcatchments with different
519 vegetation and snowpack conditions in the northern Hokkaido Island of Japan.
520 Biogeochemistry 88(1), 15-30.
521 Creed, I.F., Beall, F.D., 2009. Distributed topographic indicators for predicting nitrogen export
522 from headwater catchments, Water Resour. Res., 45, W10407, doi:10.1029/2008WR007285.
523 Creed, I.F., Band, L.E., 1998. Export of nitrogen from catchments within a temperate forest:
524 evidence for a unifying mechanism regulated by variable source area dynamics. Water Resour.
525 Res. 11, 3105-3120.
526 Creed, I.F., Band, L.E., 1996. Regulation of nitrate-N release from temperate forests: A test of the
527 N flushing hypothesis. Water Resour. Res. 32(11), 3337-3354.

528 Driscoll, C.T., Whitall, D., Aber, J.D., Boyer, E.W., Castro, M., Cronan, C., Goodale, C.L.,
529 Groffman, P.M., Hopkinson, C., Lambert, K., Lawrence, G.B., Ollinger, S.V., 2003. Nitrogen
530 pollution in the northeastern US: sources, effects, and management options. Bioscience 53,
531 357-374.
532 Galloway, J.H., Aber, J.D., Erisman, J.W., Seitzinger, S.P., Howarth, R.W., Cowling, E.B., Cosby,
533 B.J., 2003. The nitrogen cascade. Bioscience 53, 341-356.
534 Germer, S., Neill, C., Krusche, A.V., Elsenbeer, H., 2010. Influence of land-use change on
535 near-surface hydrological processes: undisturbed forest to pasture. J. Hydrol. 380, 473-480.
536 Hammermeister, D.P., Kling, G.F., Vomocil, J.A., 1982. Perched water tables on hillsides in
537 western Oregon, I. Some factors affecting their development and longevity, Soil Sci. Soc.
538 Am. J. 46 (4), 811-818.
539 Han, J.G., Li, Z.B., Li P., Tian, J.L., 2010. Nitrogen and phosphorous concentrations in runoff from
540 a purple soil in an agricultural watershed. Agri. Water Mgmt. 97, 757-762.
541 Hayakawa, A., Shimizu, M.K., Woli, K.P., Kuramochi, K., Hatano, R., 2006. Evaluating Stream
542 Water Quality through Land Use Analysis in Two Grassland Catchments: Impact of
543 Wetlands on Stream Nitrogen Concentration. J. Environ. Qual. 35, 617-627.
544 Hayakawa, A., Woli, K.P., Shimizu, M., Nomaru, K., Kuramochi, K., Hatano, R., 2009. The
545 nitrogen budget and relationships with riverine nitrogen exports of a dairy cattle farming
546 catchment in eastern Hokkaido, Japan. Soil Sci. Plant Nutr. 55, 800-819.
547 Hokkaido Government. 1996. Agriculture in Hokkaido. Hokkaido Kyodo Tsushinsha, Sapporo,
548 Japan. pp. 47 (in Japanese).
549 Inamdar, S.P., Christopher, S.F., Mitchell, M.J., 2004. Export mechanisms for dissolved organic

carbon and nitrate during storm events in a glaciated forested catchment in New York, USA. Hydrol. Process. 18, 2651-2661.

Inamdar, S.P., Mitchell, M.J., 2006. Hydrologic and topographic controls on storm-event exports of dissolved organic carbon (DOC) and nitrate across catchment scales. Water Resour. Res. 42, W03421, doi: 10.1029/2005WR004212.

Iqbal, M.Z. 2002. Nitrate flux from aquifer storage in excess of baseflow contribution during a rain event. Water Res. 36, 788-792.

Jiang, R. Woli, K.P., Kuramochi, K., Hayakawa, A., Shimizu, M., Hatano, R., 2010. Hydrological process controls on nitrogen export during storm events in an agricultural watershed. Soil Sci. Plant Nutr. 56, 72-85.

Kaushal, S.S., Groffman, P.M., Band, L.E., Band, L.E., Shields, C.A., Morgan, R.P., Palmer, M.A., Belt, K.T., Swan, C.M., Findlay, S.E.G., Fisher, G.T., 2008. Interaction between urbanization and climate variability amplifies watershed nitrate export in Maryland. Environ. Sci. Technol. 42, 5872-5878.

McDowell, R.W., Drewry, J.J., Paton, R.J., Carey, P.L., Monaghan, R.M., Condron, L.M., 2003. Influence of soil treading on sediment and phosphorus losses in overland flow. Aust. J. Soil Res. 41 (5), 949-961.

McHale, M., McDonnell, J.J., Mitchell, M.J., Cirmo, C.P., 2002. A field based study of soil- and groundwater nitrate release in an Adirondack forested watershed. Water Resour. Res. 38(4), 1029/2000 WR000102.

McNamara, J.P., Kane, D.L., Hobbie, J.E., George, W.K., 2008. Hydrologic and biogeochemical controls on the spatial and temporal patterns of nitrogen and phosphorus in the Kuparuk

River, arctic Alaska. Hydrol. Process. 22, 3294-3309.

Mitchell, M.J., Driscoll, C.T., Kahl, J.S., Likens, G.E., Murdoch, P.S., Pardo, L.H., 1996. Climatic control of nitrate loss from forested watersheds in the Northeast United States. Environ. Sci. Technol. 30, 2609-2612.

Mosley, M.P., 1982. Subsurface flow velocities through selected forest soils, South Island, New Zealand, J. Hydrol., 55, 65-92.

Ogawa, A., Shibata, H., Suzuki, K., Mitchell, M.J. and Ikegami, Y., 2006. Relationship of topography to surface water chemistry with particular focus on nitrogen and organic carbon solutes within a forested watershed in Hokkaido, Japan. Hydrol. Process. 20, 251-265.

Ou, Z., Jia, L., Jin, H., Yediler, A., Jiang, X., Kettrup, A., Sun, T., 1999. Formation of soil macropores and preferential migration of linear alkylbenzene sulfonate (LAS) in soils. Chemosphere 38(9), 1985-1996.

Park, J.H., Mitchell, M.J., McHale, P.J, Christopher, S.F., Myer, T.P., 2003. Impacts of changing climate and atmospheric deposition on N and S drainage losses from a forested watershed of the Adirondack Mountains, New York State. Global Chang. Biol. 9, 1602-1619.

Pathak, P., Wani, S.P., Singh, P., Sudi, R., 2004. Sediment flow behavior from small agricultural watersheds. Agri. Water Mgmt. 67, 105-117.

Piatek, K.B., Christopher, S.F., Mitchell, M.J., 2009. Spatial and temporal dynamics of stream chemistry in a forested watershed. Hydrol. Earth Syst. Sci., 13, 423-439.

Poor, C.J., McDonnell, J.J., 2007. The effects of land use on stream nitrate dynamics. J. Hydrol. 332, 54-68.

Rusjan, S., Brilly, M., Mikos, M., 2008. Flushing of nitrate from a forested watershed: An insight

into hydrological nitrate mobilization mechanisms through seasonal high-frequency stream nitrate dynamics. J. Hydrol. 354, 187-202.

Shanley, J.B., Chalmers, A., 1999. The effect of frozen soil on snowmelt runoff at Sleepers River, Vermont. Hydrol. Process. 13, 1843-1857.

Shibata, H., Kuraji, K., Toda, H., Sasa, K., 2001. Regional comparison of nitrogen export to Japanese forest streams, in: Optimizing nitrogen management in food and energy production and environmental protection: proceedings of the 2nd international nitrogen conference on science and policy. Sci. World 1(S2), 572-580.

Tachibana, H., Nasu, Y., 2003. Measurement of runoff, In: The Japan Society for Analytical Chemistry, Hokkaido Branch (Ed.), Water Analysis, Kagaku Dojin, Kyoto, pp. 362-370 (in Japanese).

Takeuchi, M., 1980. Studies on the freezing and thawing of the volcanic ash soils in eastern Hokkaido. I. The seasonal aspects of the freezing and thawing in a plowed field. Bull. Kyoto Univ. Forests 52, 117-129 (in Japanese with English summary).

Takeuchi, M., 1981. Studies on the freezing and thawing of the volcanic ash soils in eastern Hokkaido. II. Soil freezing and thawing in a grassland (Sasa nipponica) and a brush cutting area. Bull. Kyoto Univ. Forests 53, 205-215 (in Japanese with English summary).

Vidon, P., Hubbard, L.E., Soyeux, E., 2009. Seasonal solute dynamics across land uses during storms in glaciated landscape of the US Midwest. J. Hydrol. 376, 34-47.

Wagner, L.E., Vidon, P., Tedesco, L.P., Gray, M., 2008. Stream nitrate and DOC dynamics during three spring storms across land uses in glaciated landscapes of the Midwest. J. Hydrol. 362, 177-190.

616 Welsch, D.L., Kroll, C.N., McDonnell, J.J., Burns, D.A., 2001. Topographic controls on the
617 chemistry of subsurface stormflow. Hydrol. Process. 15, 1925-1938.
618 Woli, K.P., Nagumo, T., Hatano, R., 2002. Evaluating impact of land use and N budgets on stream
619 water quality in Hokkaido, Japan. Nut. Cyc. Agroecosys. 63, 175-184.
620 Woli, K.P., Nagumo, T., Kuramochi, K., Hatano, R., 2004. Evaluating river water quality through
621 land use analysis and N budget approaches in livestock farming areas. Sci. Total Environ.
622 329, 61-74.
623 Zhang, Z., Fukushima, T., Onda, Y., Gomi, T., Fukuyama, T., Sidle, R., Kosugi, K., Matsushige,
624 K., 2007. Nutrient runoff from forested watersheds in central Japan during typhoon storms:
625 implications for understanding runoff mechanisms during storm events. Hydrol. Process. 21,
626 1167-1178.

Table
Click here to download Table: table-submit.doc

659 Table 1 Land use and topographic characteristics for the three headwater stream watersheds

Watershed	Area (km^2)	Land use (%)		Slope (%)			Relief ratio
		Agriculture	Forest	0-5	5-10	10-100	
AW	14.3	73.5	23.5	86.0	11.6	2.4	0.0146
AFW	36.6	58.9	37.1	60.2	19.5	20.3	0.0362
FW	70.0	14.5	84.4	17.0	20.2	62.8	0.0553

660

661 AW: agricultural watershed; AFW: mixed agriculture-forested watershed; FW: forested watershed

662

663 Table 2 Climatic conditions of the Shibetsu watershed during the study period

	Rainfall (mm)		Annual snowfall (cm)	Maximum snowpack depth (cm)
	Annual	Maximum daily rainfall		
2003	1,276	106	626	71
2004	931	49	612	109
2005	975	99	384	83
30-yr average	1,147	89	480	71

664

	Rainfall (mm)		Annual snowfall (cm)	Maximum snowpack depth (cm)
	Annual	Maximum daily rainfall		
2003	1276	106	626	71
2004	931	49	612	109
2005	975	99	384	83
30-yr average	1147	89	480	71

665

666

667 Table 3 Characteristics of the rainfall events in 2003

Rainfall event	Rainfall		API_X		RC			Watershed
	Total (mm)	Maximum intensity (mm h^{-1})	API_{21}	API_7	FW	AFW	AW	
20 Jun 2003	80	13	5.19	3.24		0.08		AFW
10 Jul 2003	91	11	6.03	0.00	0.16			FW
30 Jul 2003	44	7	6.11	0.17		0.11	0.09	AFW; AW
8 Aug 2003	20	5	7.24	2.03	0.24	0.11	0.08	FW; AFW; AW
25 Aug 2003	16	7	16.33	2.00	0.49	0.26		FW; AFW
9 Sep 2003	31	9	5.62	3.67		0.13	0.09	AFW; AW
19 Sep 2003	15	9	13.56	8.55		0.25		AFW
26 Sep 2003	34	9	28.81	23.45		0.13		AFW
23 Oct 2003	50	10	2.64	1.90			0.07	AW
18 Jul 2004	10	8	2.42	0.86			0.19	AW
30 Aug 2004	28	7	9.30	0.58	0.22			FW
7 Sep 2004	27	6	7.97	4.14	0.17		0.09	FW; AW
15 Nov 2004	15	8	28.22	24.18	0.14			FW
26 Jul 2005	76	11	2.71	0.33	0.06			FW

API_X: antecedent precipitation index for 7 and 21 days before a rainfall event, respectively; RC: runoff coefficient; AW: agricultural watershed; AFW: mixed agriculture-forested watershed; FW: forested watershed.

Table 4 The time in multiple of T*p* and the NO_3^--N concentration when NO_3^--N peaked

Watershed	Rainfall event	Time to peak discharge rate (T*p*) (h)	Time in multiple of T*p* at NO_3^--N peak [a]	NO_3^--N peak concentration (mg L^{-1}) [b]
FW	10 Jul 2003	9.0	1.0	0.50
	8 Aug 2003	6.0	0.7	0.31
	25 Aug 2003	2.5	1.0	0.32
	30 Aug 2004	5.0	0.8	0.44
	7 Sep 2004	6.0	0.7	0.50
	15 Nov 2004	5.0	0.6	0.59
	26 Jul 2005	3.75	0.5	0.80
AFW	20 Jun 2003	7.0	3.3	1.29
	30 Jul 2003	6.75	1.3	1.17
	8 Aug 2003	5.0	3.0	1.10
	25 Aug 2003	2.0	1.0	1.22
	9 Sep 2003	7.0	2.1	1.07
	19 Sep 2003	2.0	1.3	1.08
	26 Sep 2003	1.5	7.3	1.76
AW	30 Jul 2003	5.0	1.8	1.77
	8 Aug 2003	5.0	1.8	1.86
	9 Sep 2003	6.0	8.0	1.98
	23 Oct 2003	27.0	1.0	1.91
	18 Jul 2004	5.0	1.5	1.80
	7 Sep 2004	7.0	2.1	1.62

674 [a] The time in multiples of T*p* when the largest peak concentration of NO_3^--N occurred; [b] The largest peak
675 concentration of NO_3^--N during a rainfall event. AW: agricultural watershed; AFW: mixed agriculture-forested
676 watershed; FW: forested watershed.

Figure1

Click here to download high resolution image

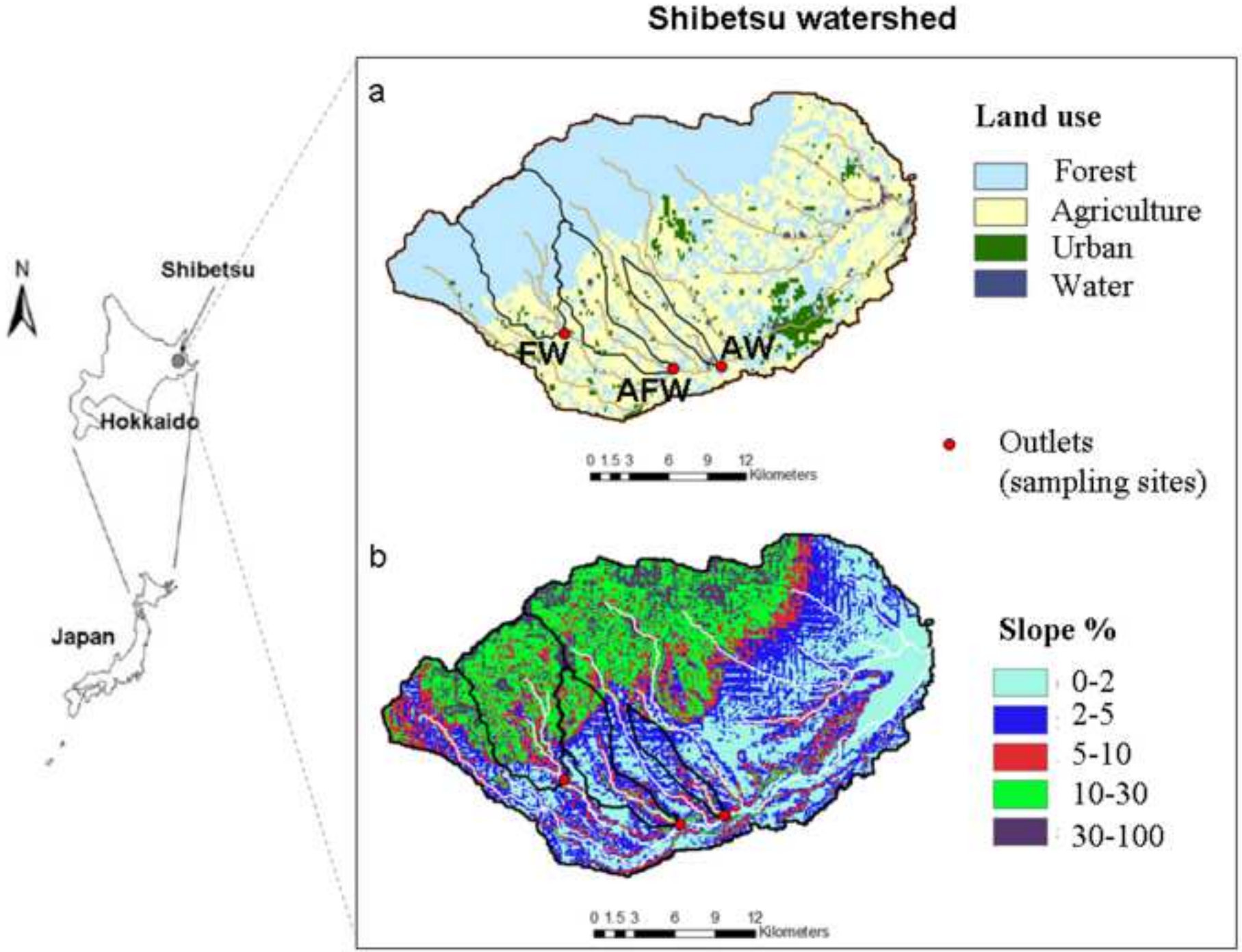

Figure 2

Click here to download high resolution image

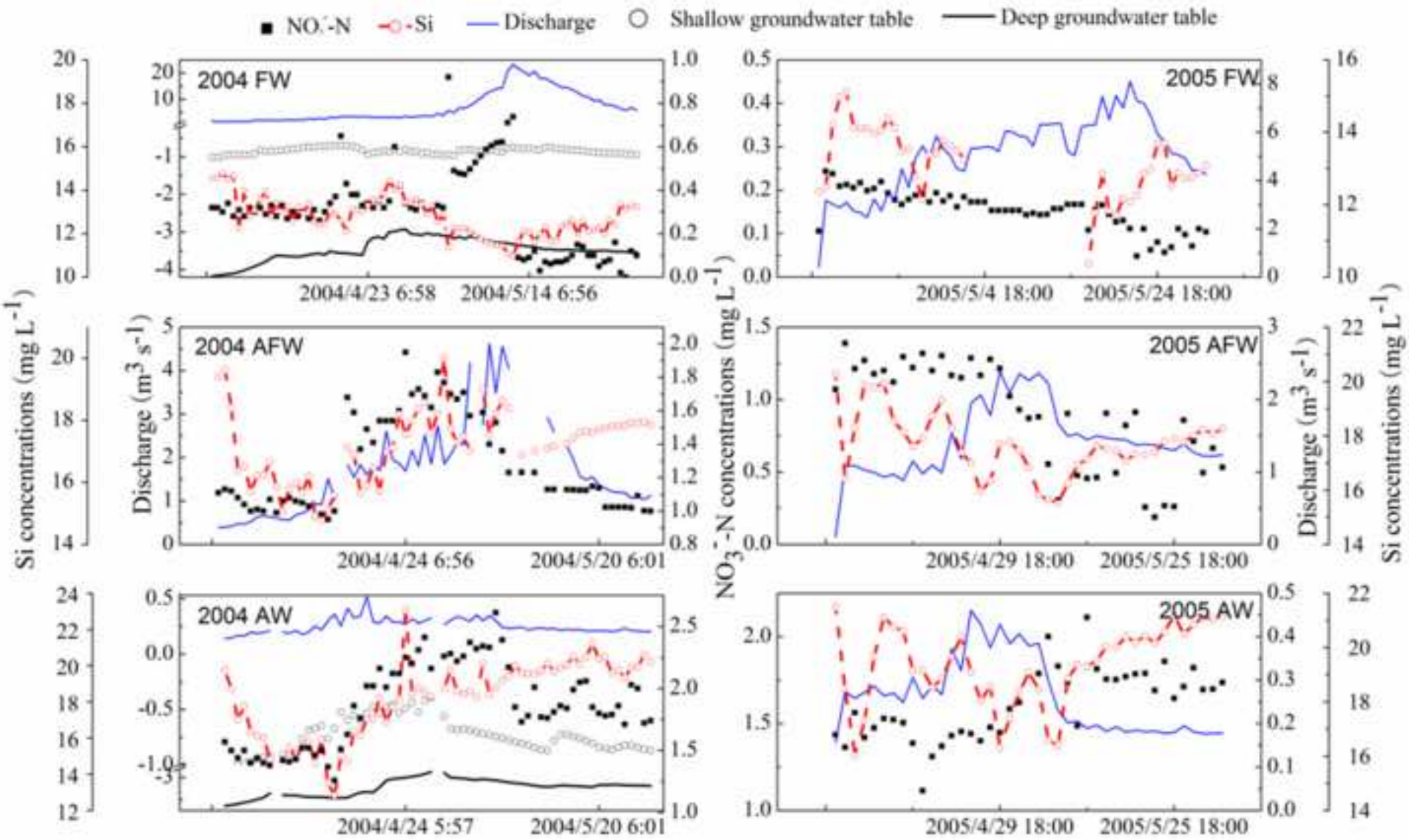

Figure3a

Click here to download high resolution image

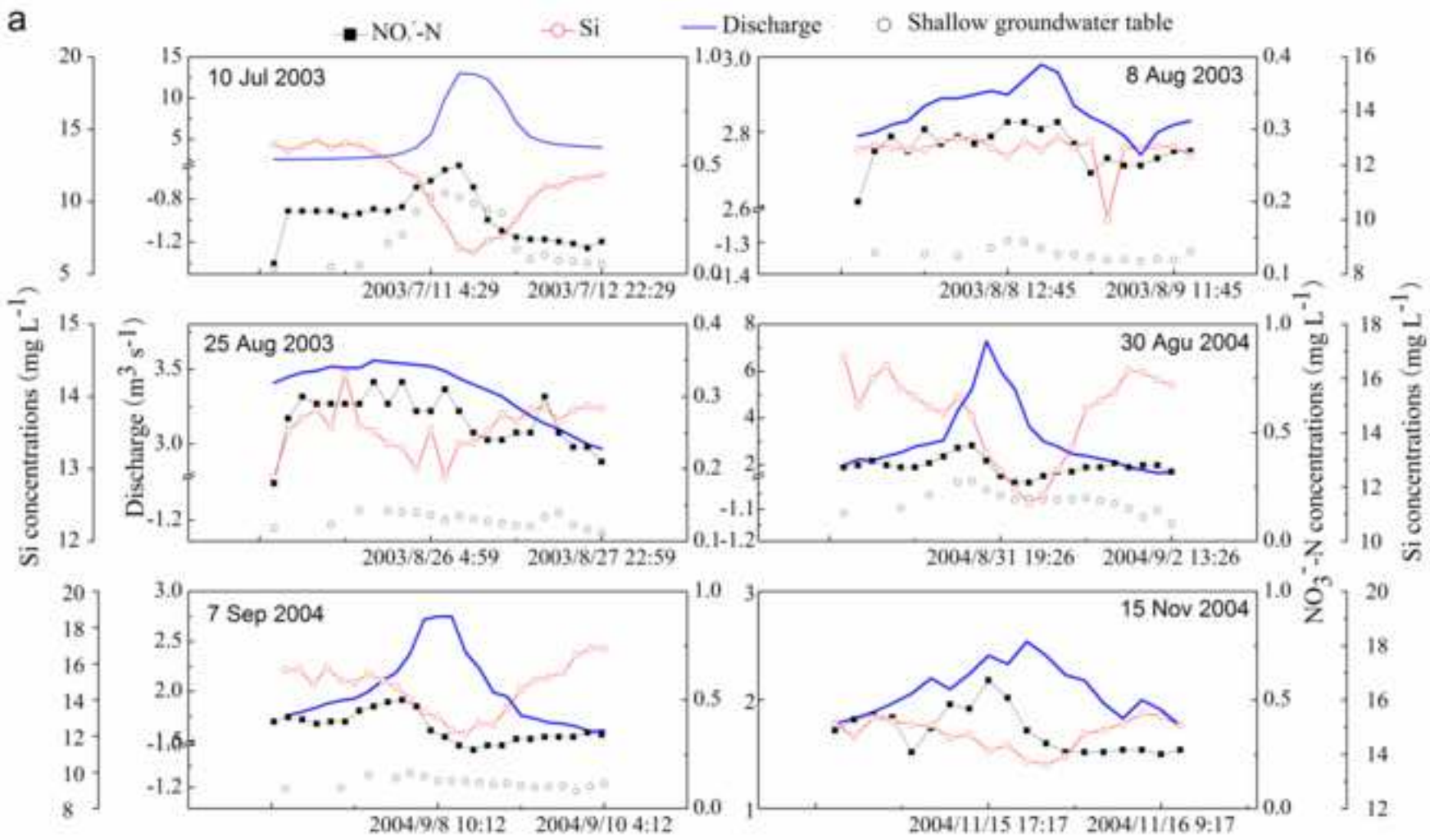

Figure3b

Click here to download high resolution image

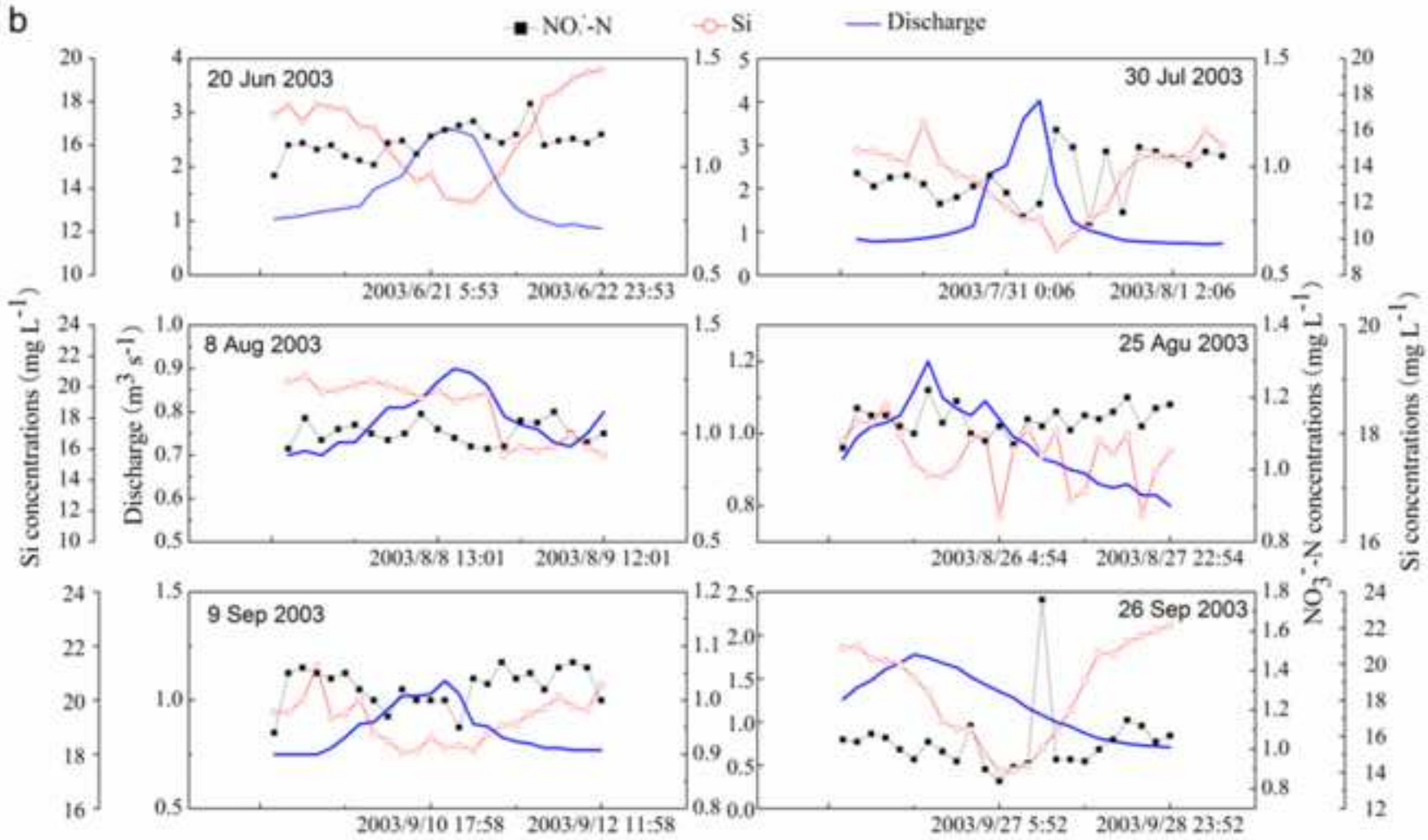

Figure3c

Click here to download high resolution image

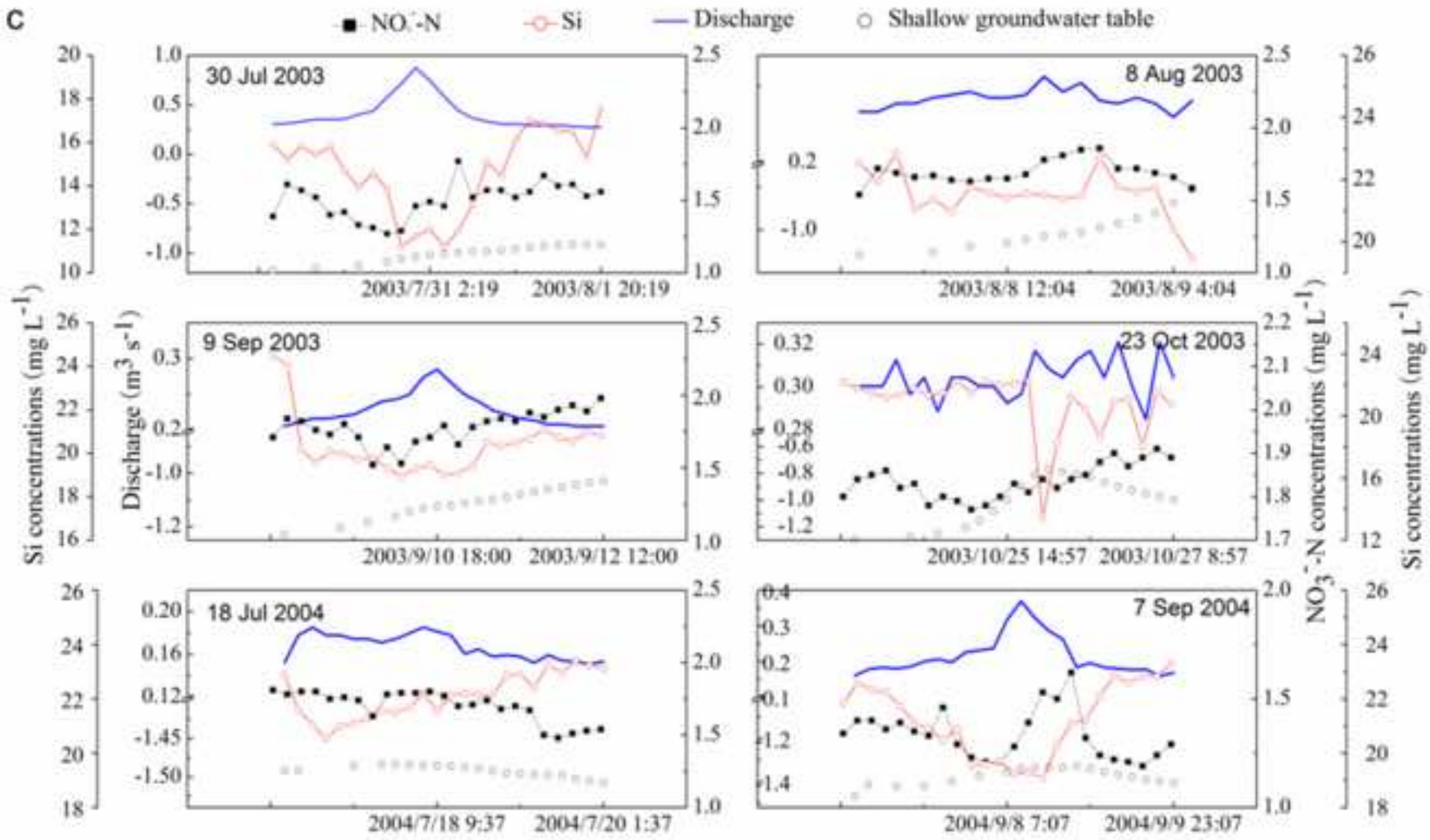

Figure4

Click here to download high resolution image

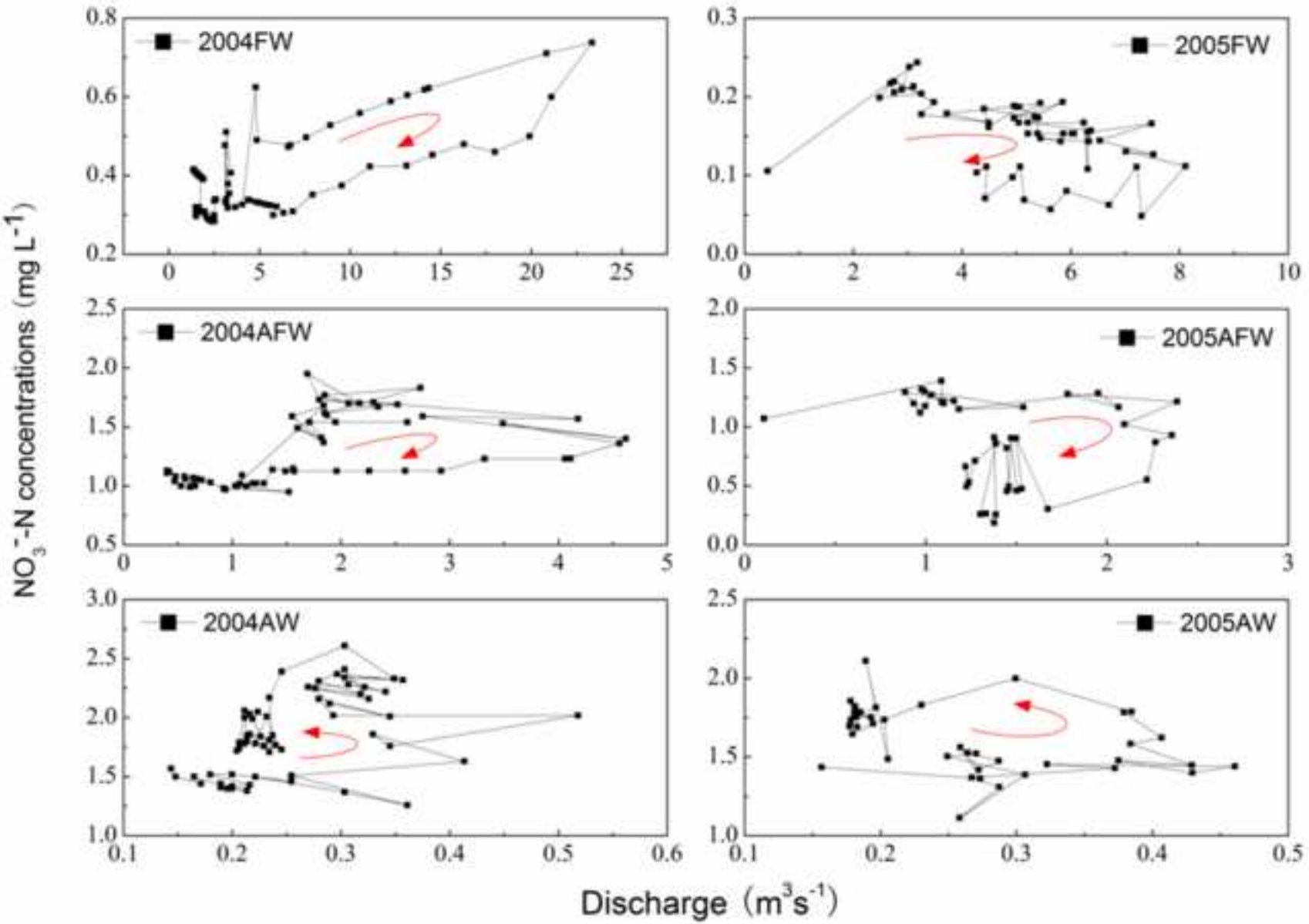

Figure5a

Click here to download high resolution image

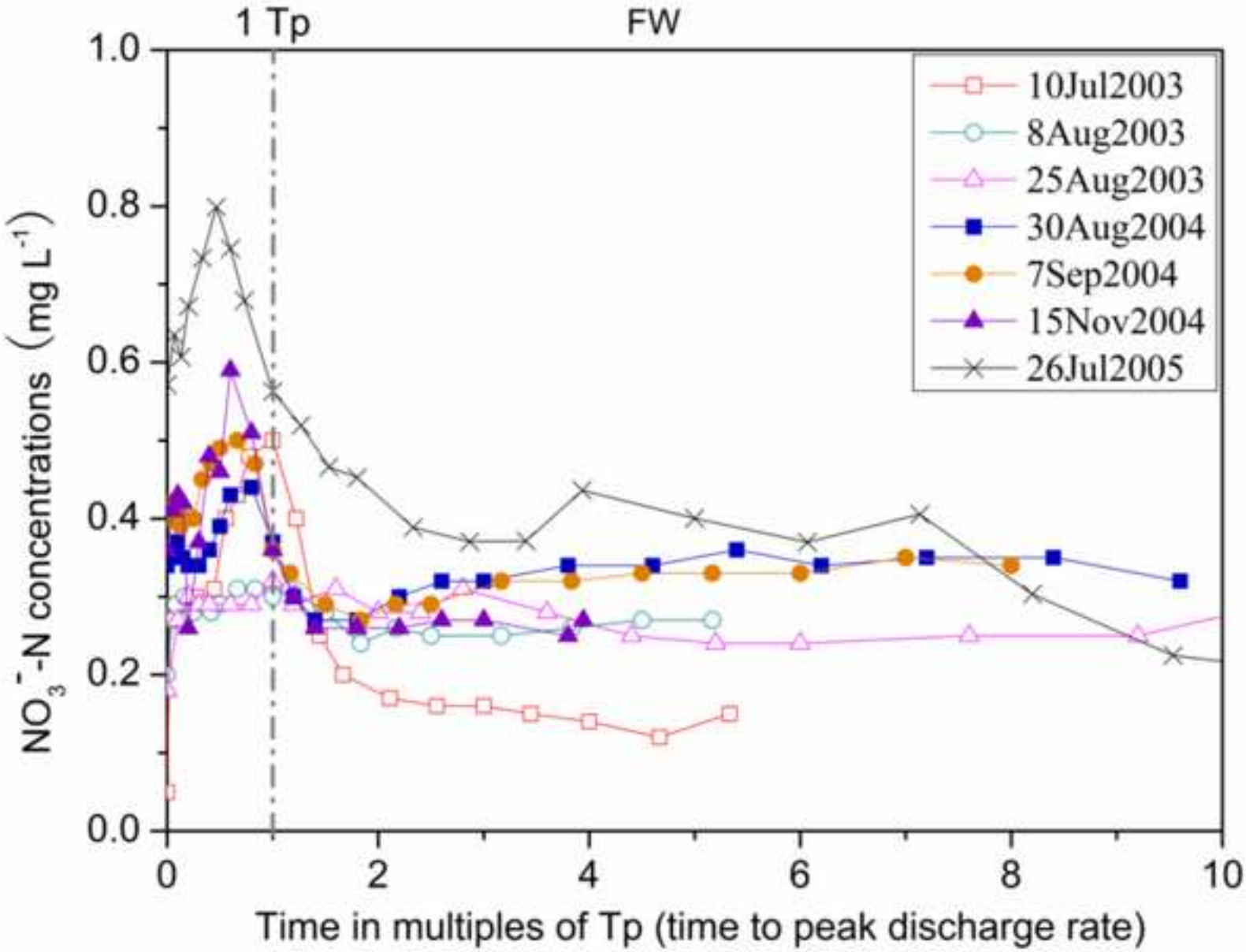

Figure5b

Click here to download high resolution image

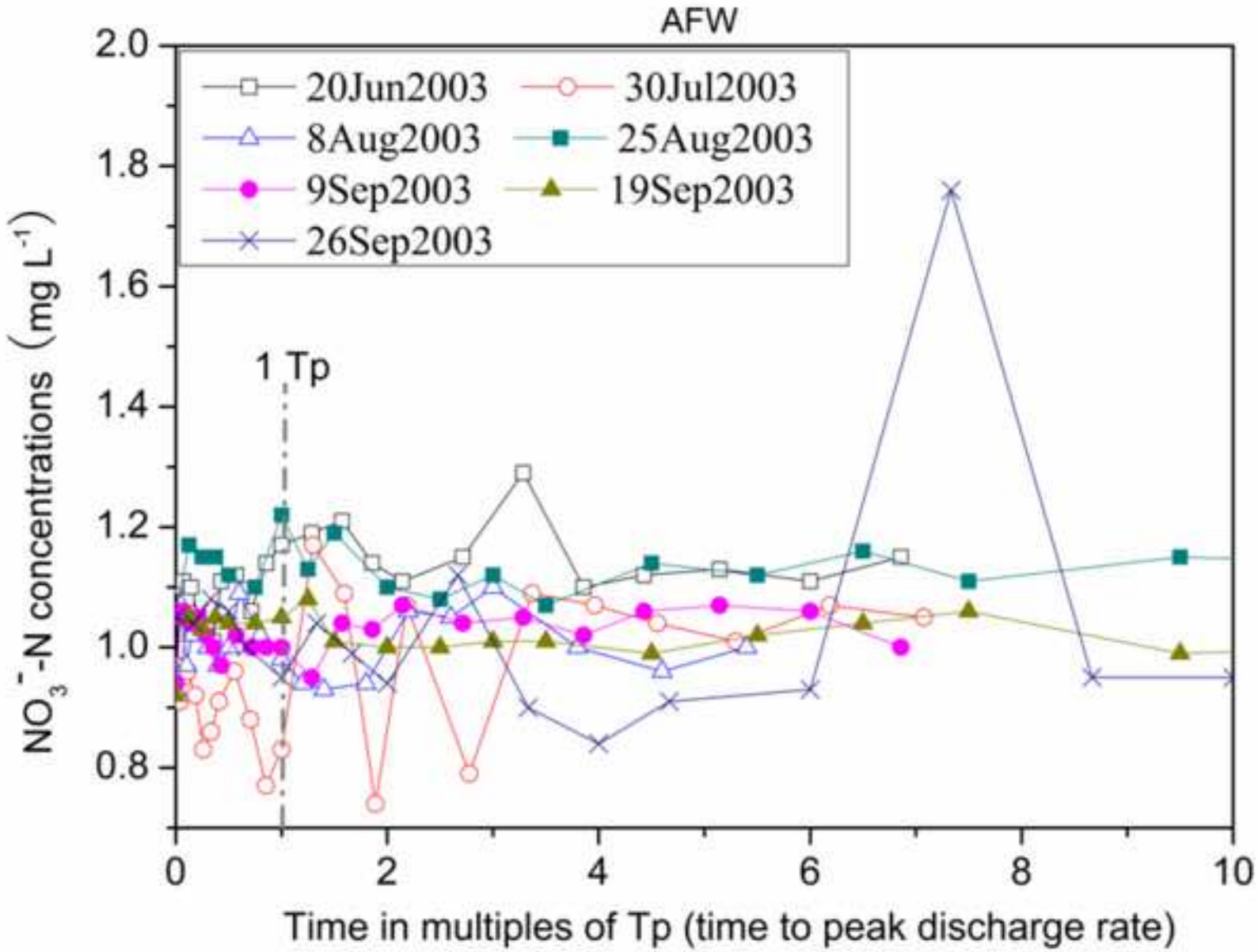

Figure5c

Click here to download high resolution image

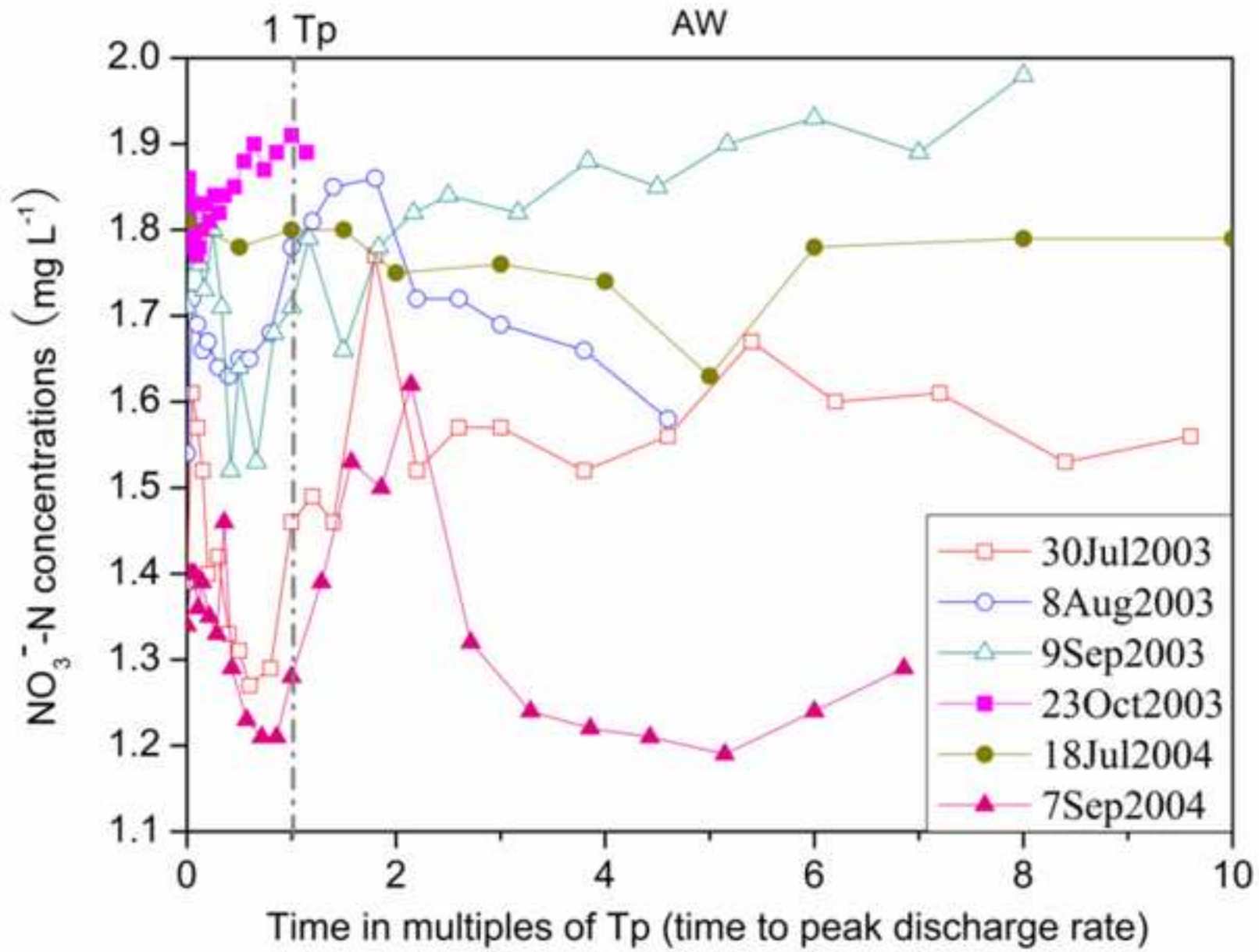

Figure 6

Click here to download high resolution image

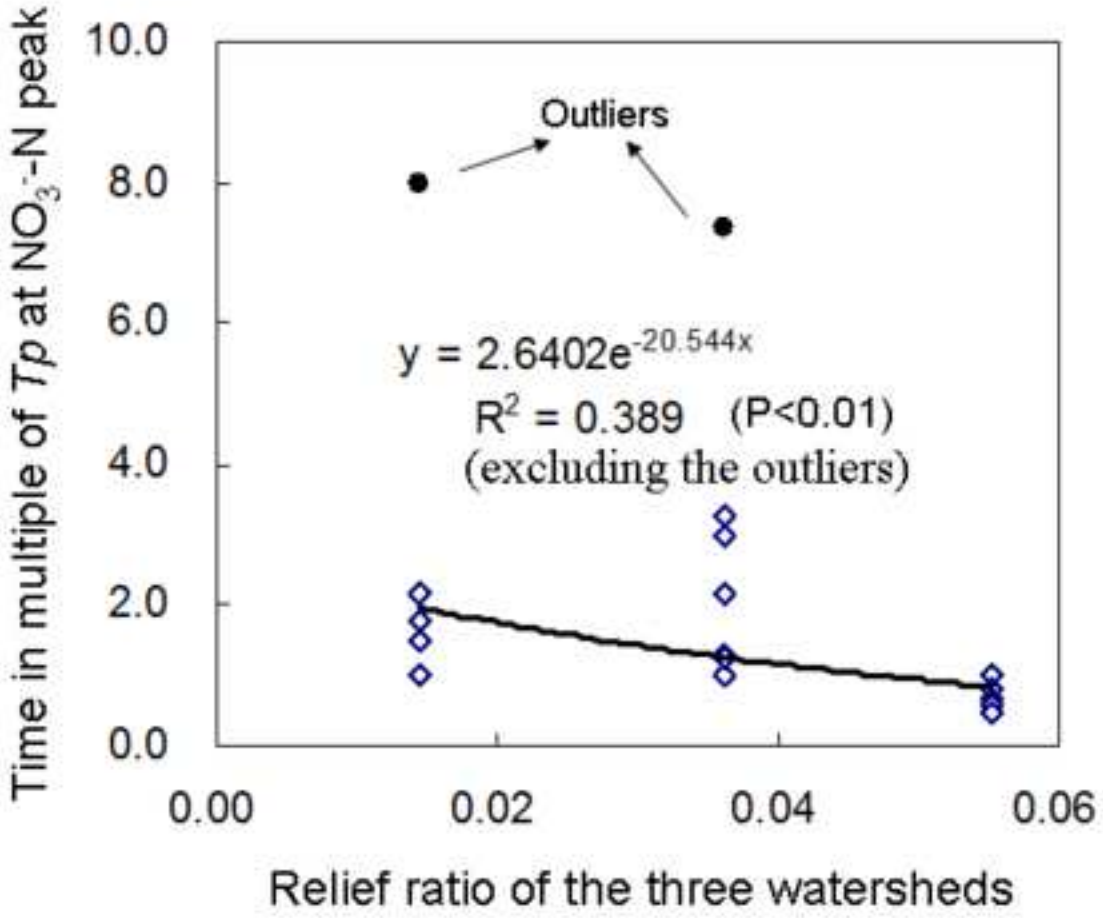

Figure7

Click here to download high resolution image

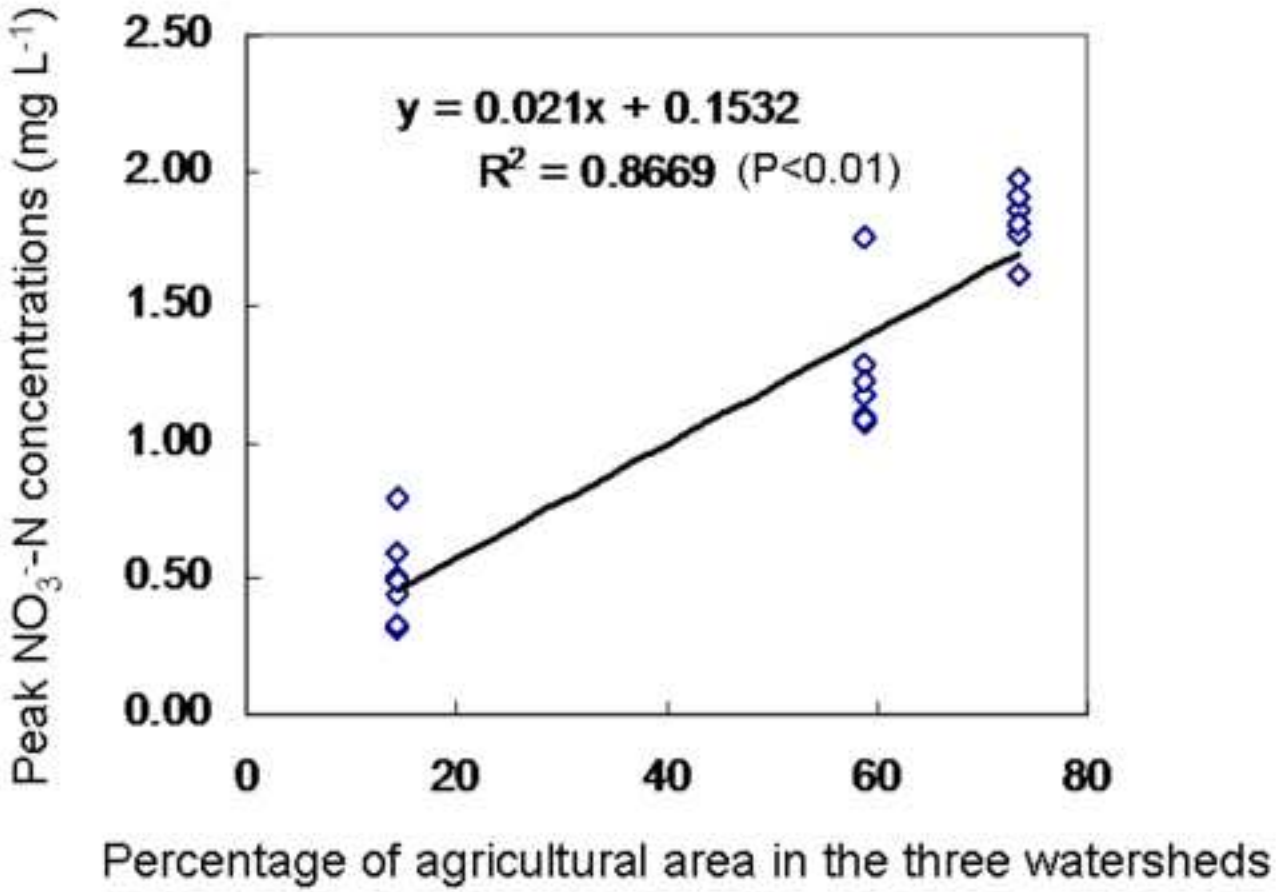

677 **Figure captions**

678 Figure 1. Locations of the watersheds and the sampling sites and the coupled land use and
679 topography characteristics

680 Figure 2. Time-series of the discharge, groundwater table, NO_3^--N and Si concentrations during
681 snowmelt season in 2004 and 2005 (AW: agricultural watershed, AFW: mixed
682 agriculture-forested watershed, FW: forested watershed)

683 Figure 3. Time-series of discharge, shallow groundwater table, NO_3^--N and Si concentrations
684 during selected rainfall events in (a) forested watershed: FW, (b) mixed agriculture-forested
685 watershed: AFW, (c) agricultural watershed: AW

686 Figure 4. Relationships between discharge and NO_3^--N concentrations during the snowmelt season
687 in 2004 and 2005 in the agricultural, mixed agriculture-forested, and forested watersheds
688 (AW, AFW and FW, respectively)

689 Figure 5. The dynamics of NO_3^--N concentrations as a function of the time to peak discharge rates
690 for different rainfall events in the forested watershed (FW), mixed agriculture-forested
691 watershed (AFW) and agricultural watershed (AW)

692 Figure 6. The relationship between the watershed relief ratio and the time in multiples of T*p* of the
693 NO_3^--N peak during rainfall events

694 Figure 7. The relationship between the percentage of agricultural area in the watershed and the
695 peak NO_3^--N concentrations during rainfall events